1521-009X/43/7/1061–1070$25.00
Drug Metabolism and Disposition

http://dx.doi.org/10.1124/dmd.114.061440
Drug Metab Dispos 43:1061–1070, July 2015

# Upregulation of UGT2B4 Expression by 3′-Phosphoadenosine-5′-Phosphosulfate Synthase Knockdown: Implications for Coordinated Control of Bile Acid Conjugation[S]

Kathleen G. Barrett, Hailin Fang, Daniela Cukovic, Alan A. Dombkowski, Thomas A. Kocarek, and Melissa Runge-Morris

*Institute of Environmental Health Sciences, Wayne State University, Detroit, Michigan (K.G.B., H.F., T.A.K., M.R.-M.); and Department of Pediatrics, Wayne State University, Detroit, Michigan (D.C., A.A.D.)*

Received October 13, 2014; accepted May 6, 2015

## ABSTRACT

**During cholestasis, the bile acid–conjugating enzymes, SULT2A1 and UGT2B4, work in concert to prevent the accumulation of toxic bile acids. To understand the impact of sulfotransferase deficiency on human hepatic gene expression, we knocked down 3′-phosphoadenosine-5′-phosphosulfate synthases (PAPSS) 1 and 2, which catalyze synthesis of the obligate sulfotransferase cofactor, in HepG2 cells. PAPSS knockdown caused no change in SULT2A1 expression; however, UGT2B4 expression increased markedly (~41-fold increase in UGT2B4 mRNA content). Knockdown of SULT2A1 in HepG2 cells also increased UGT2B4 expression. To investigate the underlying mechanism, we transfected PAPSS-deficient HepG2 cells with a luciferase reporter plasmid containing ~2 Kb of the UGT2B4 5′-flanking region, which included a response element for the bile acid–sensing nuclear receptor, farnesoid X receptor (FXR). FXR activation or overexpression increased UGT2B4 promoter activity; however, knocking down FXR or mutating or deleting the FXR response element did not significantly decrease UGT2B4 promoter activity. Further evaluation of the UGT2B4 5′-flanking region indicated the presence of distal regulatory elements between nucleotides −10090 and −10037 that negatively and positively regulated UGT2B4 transcription. Pulse-chase analysis showed that increased UGT2B4 expression in PAPSS-deficient cells was attributable to both increased mRNA synthesis and stability. Transfection analysis demonstrated that the UGT2B4 3′-untranslated region decreased luciferase reporter expression less in PAPSS-deficient cells than in control cells. These data indicate that knocking down PAPSS increases UGT2B4 transcription and mRNA stability as a compensatory response to the loss of SULT2A1 activity, presumably to maintain bile acid–conjugating activity.**

## Introduction

Cytosolic sulfotransferases (SULTs) and UDP-glucuronosyltransferases (UGTs) are biotransformation enzymes that catalyze the conjugation of a variety of xenobiotics and endogenous compounds to sulfonate or glucuronate moieties. SULTs and UGTs recognize similar substrates and are regulated by nuclear signaling pathways involved in normal metabolic processes, suggesting some coordinated action. For example, SULT2A1 and UGT2B4 metabolize steroids and bile acids (BAs) and play important roles in BA homeostasis. Due to the cytotoxic properties of BAs, bile homeostasis is a tightly regulated process. During pathophysiological conditions where bile flow is obstructed (i.e., cholestasis), urinary elimination of BAs increases to circumvent the accumulation of intracellular BAs and liver damage, and more urinary BAs are in the sulfonated and glucuronidated forms (van Berge Henegouwen et al., 1976; Takikawa et al., 1986; Pillot et al., 1993). Under these conditions enhanced metabolism by SULT2A1 and UGT2B4 acts as a defensive mechanism preventing BA cytotoxicity.

Recently, we reported the upregulation of hepatic Sult2a1 in hyposulfatemic NaS1 null mice (Barrett et al., 2013). These mice are unable to reabsorb sulfate and display physiologic alterations that include elevated serum BA levels and altered hepatic lipid metabolism (Dawson et al., 2003, 2006). We hypothesized that Sult2a1 upregulation in NaS1 null mice was attributable to reduced hepatic sulfotransferase activity, resulting in increased levels of BAs able to activate the BA-sensing farnesoid X receptor (FXR) in an attempt to restore BA homeostasis (Barrett et al., 2013). To investigate this regulatory mechanism, a human liver cell model with diminished sulfonation capacity was created by knocking down 3′-phosphoadenosine-5′-phosphosulfate (PAPS) synthases (PAPSS) 1 and 2 in HepG2 cells (shPAPSS1/2 cells) (Barrett et al., 2013). The suppression of PAPSS1 and 2 would decrease the levels of obligate cofactor and sulfate donor PAPS and reduce cellular sulfotransferase activity (Klaassen and Boles, 1997). Higher mouse Sult2a1 promoter activity was observed when reporter

This research was supported by the National Institutes of Health National Institute of Environmental Health Sciences [Grant R01 ES005823 (to M.R.-M.) and Center Grant P30 ES020957].

dx.doi.org/10.1124/dmd.114.061440.

[S]This article has supplemental material available at dmd.aspetjournals.org.

**ABBREVIATIONS:** BA, bile acid; DMEM, Dulbecco's modified Eagle's medium; EU, ethynyl uridine; FXR, farnesoid X receptor; FXRE, farnesoid X receptor response element; GW4064, 3-(2,6-dichlorophenyl)-4-(3′-carboxy-2-chlorostilben-4-yl)oxymethyl-5-isopropylisoxazole; HDCA, hyodeoxycholic acid; HRP, horseradish peroxidase; LCA, lithocholic acid; LS, linker scanning; NT, non-targeting; PAPS, 3′-phosphoadenosine-5′-phosphosulfate; PAPSS, 3′-phosphoadenosine-5′-phosphosulfate synthase; qRT-PCR, quantitative reverse transcription–polymerase chain reaction; siRNA, small interfering RNA; SULT, cytosolic sulfotransferase; UGT, UDP-glucuronosyltransferase; 3′-UTR, 3′-untranslated region.

constructs containing an intact inverted repeat of AGGTCA with zero intervening nucleotide motifs were transiently transfected into the shPAPSS1/2 cells compared with control cells. However, a species difference was noted in that endogenous SULT2A1 was not upregulated in PAPSS1/2 double knockdown HepG2 cells, whereas the amount of UGT2B4 mRNA was significantly increased. UGT2B4 is the predominant UGT in human liver that conjugates BAs and is a known target of FXR (Pillot et al., 1993; Barbier et al., 2003; Izukawa et al., 2009; Ohno and Nakajin, 2009; Court et al., 2012). The upregulation of UGT2B4 may be a human-specific compensatory response to the loss of BA sulfonation to prevent liver damage in the event of sulfate depletion. In this study we investigate the mechanism(s) responsible for the PAPSS1/2 knockdown-mediated upregulation of human UGT2B4.

## Materials and Methods

**Cell Culture.** HepG2 cells were engineered for stable knockdown of PAPSS1 and PAPSS2 (shPAPSS1/2 cells) or SULT2A1 (shSULT2A1 cells), or for stable expression of a non-targeting shRNA (shNT cells), as described previously (Barrett et al., 2013). Cells were cultured in Dulbecco's modified Eagle's medium (DMEM) supplemented with nonessential amino acid mix, 100 U/ml penicillin, 100 $\mu$g/ml streptomycin, and 10% fetal bovine serum (all purchased from Life Technologies, Grand Island, NY). Cells were maintained under a humidified atmosphere of 95% air, 5% $CO_2$ at 37°C.

**Microarray Analysis.** Total RNA was prepared from four independent batches of cultured HepG2 (shNT and shPAPSS1/2) cells using the RNeasy Mini Kit (Qiagen, Valencia, CA) and evaluated for quality using a 2100 Bioanalyzer (Agilent Technologies, Santa Clara, CA). The RNA samples were labeled with Alexa 647 or Alexa 555, using the Agilent Low Input Fluorescent Linear Amplification Kit. Microarray analysis was performed using Human v.2. GE 4x44K Microarrays (Agilent Technologies), using a basic two-color hybridization design to determine relative gene expression levels in shPAPSS1/2 versus shNT samples. Dye swaps were performed to account for dye bias effects such that for the four arrays, in two of the arrays the shNT samples were labeled with Alexa 647 and the shPAPSS1/2 samples were labeled with Alexa 555, while in the other two arrays the dye orientation was reversed. Microarrays were scanned using the Agilent dual laser DNA microarray scanner, model G2565AA, and image analysis was performed using Agilent Feature Extraction software. Outlier features having aberrant image characteristics were flagged and excluded from subsequent analysis. Fluorescent intensity values were adjusted using local background subtraction. For each probe on the array, a log 2 ratio was calculated, representing the relative abundance of transcript in shPAPSS1/2 cells relative to shNT cells. Statistical analyses of microarray data were performed using GeneSpring, version 7.3 (Agilent Technologies). The data from the four replicate arrays were analyzed using *t* tests (against zero) and the Benjamini and Hochberg multiple test correction to control the false discovery rate to 5%.

**Quantitative Reverse Transcription–Polymerase Chain Reaction (qRT-PCR) Analysis of UGT2B4 and SULT2A1 Expression.** Total RNA was prepared from cultured HepG2 clones using the Purelink RNA Mini Kit (Ambion/Life Technologies). RNA (1.5 $\mu$g) was reverse transcribed to cDNA using the High Capacity cDNA Reverse Transcription Kit according to the manufacturer's instructions (Life Technologies). UGT2B4 and SULT2A1 mRNA levels were measured using TaqMan Gene Expression Assays Hs00607514_mH and Hs00234219_m1, respectively (Life Technologies) and a StepOnePlus Real Time PCR System (Applied Biosystems/Life Technologies) as previously described (Barrett et al., 2013).

**Western Blot Analysis of SULT2A1 and UGT2B4.** Whole cell lysates were prepared as previously described (Rondini et al., 2014). Protein concentrations were quantified using the bicinchoninic acid protein assay according to the manufacturer's instructions (Thermo Fisher, Rockford, IL). Lysate proteins (15–30 $\mu$g) were resolved by SDS-PAGE, using 10% or 12.5% acrylamide gels and transferred onto polyvinylidene difluoride membranes. For SULT2A1, membranes were developed using a mouse monoclonal anti-SULT2A1 antibody (clone 4D7; Origene, Rockville, MD) diluted 1:5000 followed by horseradish peroxidase (HRP)–conjugated goat anti-mouse IgG (sc-2005; Santa Cruz Biotechnology, Santa Cruz, CA) diluted 1:20,000. The blots were reprobed with goat polyclonal $\beta$-tubulin antibody (ab21057; Abcam, Cambridge, MA) diluted 1:1000 followed by HRP-conjugated donkey anti-goat IgG (sc-2020; Santa Cruz Biotechnology) diluted 1:8000 or with mouse monoclonal $\alpha$-tubulin antibody (sc-5286, Santa Cruz Biotechnology) diluted 1:250 followed by HRP-conjugated goat anti-mouse IgG diluted 1:5000. UGT2B4 was detected using rabbit polyclonal anti-UGT2B4 antibody (15425 1-AP; Proteintech, Chicago) diluted 1:750 followed by HRP-conjugated goat anti-rabbit IgG (sc-2030; Santa Cruz Biotechnology) diluted 1:20,000. The blot was reprobed with mouse monoclonal anti-$\beta$-actin (clone AC15; Sigma-Aldrich, St. Louis, MO) diluted 1:30,000 or 1:40,000 followed by HRP-conjugated goat anti-mouse IgG (sc-2005; Santa Cruz Biotechnology) diluted 1:75,000. Immunoreactive proteins were detected by enhanced chemiluminescence and visualized on X-ray film. Band densities were determined using AlphaView software (Protein Simple, San Jose, CA). Data are reported as mean ratios of UGT2B4/$\beta$-actin ± S.E.M.

**Preparation of UGT2B4 Reporter Plasmids.** A fragment spanning from ~2 Kb upstream to 13 nucleotides downstream of the UGT2B4 transcription start site (considered as the 5′ position of NCBI RefSeq NM_021139.2) was amplified by PCR using Herculase II Fusion Enzyme (Agilent Technologies) and genomic DNA from MCF10A cells as template. The primer set used is listed in Supplemental Table 1. The amplified ~2 Kb fragment was digested with XhoI and BglII and ligated into the promoterless pGL4.10 [*luc2*] luciferase reporter vector (Promega Corporation, Madison, WI), resulting in the (−1991:+13)-UGT2B4-Luc reporter plasmid. This plasmid served as the template to create a series of deletion constructs containing nucleotides −1648:+13, −1119:+13, −804:+13, −484:+13, and −112:+13 (primer sets are listed in Supplemental Table 1).

Reporter constructs containing a series of upstream fragments (~2000 nucleotides each) of the UGT2B4 gene 5′-flanking region extending ~16 Kb upstream of the transcription start site were prepared from genomic DNA using PCR (primer sets listed in Supplemental Table 1). After PCR, fragments were digested with SacI and XhoI and ligated into the construct (−112:+13)-UGT2B4-Luc, which provided UGT2B4 core promoter elements. Additional deletion constructs were prepared using the primer sets, plasmid templates, and oligonucleotide pairs indicated in Supplemental Table 1. Preparation of a FXR response element (FXRE) reporter plasmid (FXRE-Luc) has been described previously (Kocarek and Mercer-Haines, 2002).

**Site-Directed Mutagenesis of FXRE.** A FXRE located at nucleotides −1193 to −1187 of the UGT2B4 5′-flanking region (Barbier et al., 2003) was mutated using (−1991:+13)-UGT2B4-Luc as the template and the QuikChange II XL site-directed mutagenesis kit (Agilent Technologies) according to the manufacturer's instructions. The mutagenic primers are listed in Supplemental Table 1.

**Preparation of Linker Scanning (LS) Mutants of the (−10503:−10037)(−112:+13)-UGT2B4-Luc plasmid.** LS mutants spanning nucleotides −10090 to −10037 in fragment (−10503:−10037) (Supplemental Fig. 1) were prepared using the method described by Gustin and Burk (2000), replacing successive six nucleotide sections with BamHI sites (GGATCC). Briefly, three PCR reactions were performed for each mutant. Initially, PCR reactions 1 and 2 were performed using LS primers 1 and 2 or LS primers 3 and 4 (Supplemental Table 1), respectively, the (−10503:−10037)(−112:+13)-UGT2B4-Luc plasmid as the template, and HotStar HiFidelity DNA polymerase (Qiagen). Each product from PCR reactions 1 and 2 was gel purified and digested with BamHI, and the digested products were combined and ligated together. The ligated product then served as the template for the third PCR reaction using primers 1 and 4. The final 662 nucleotide fragment was gel purified, digested with SacI and HindIII, and ligated into the SacI/HindIII-digested and gel-purified pGL4.10 [*luc2*] luciferase reporter vector. The sequences of all reporter constructs were verified using the services of the Wayne State University Applied Genomics Technology Center (Detroit, MI).

**Preparation of UGT2B4-3′-Untranslated Region (3′-UTR) Reporter Plasmid.** The SMARTer RACE cDNA Amplification Kit (Clontech, Mountain View, CA) was used to clone the 3′-region of the UGT2B4 mRNA sequence including 155 nucleotides of the coding region and the entire 3′-UTR (UGT2B4 gene-specific primer listed in Supplemental Table 1). RNA isolated from shPAPSS1/2 cells served as the template. The blunt ends of the PCR product were modified by A-Tailing with GoTaq DNA Polymerase according to the manufacturer's instructions (Promega), and the modified fragment was ligated into pGEM-T Easy (Promega). This vector served as the template to

amplify the UGT2B4 3′-UTR specifically using Herculase II Fusion Enzyme. The primer set used is listed in Supplemental Table 1. The fragment was digested with SacI and XhoI and ligated into the pmirGLO Dual-Luciferase miRNA Target Expression Vector (Promega), resulting in the UGT2B4-3′-UTR/Luc reporter plasmid. Computational analysis of the UGT2B4 3′-UTR for predicted micro-RNA binding sites was performed using 10 algorithms available through miRWalk (Dweep et al., 2011) (http://www.umm.uni-heidelberg.de/apps/zmf/mirwalk/predictedmirnagene.html).

**Transient Transfection Analysis.** Approximately 250,000 shNT and shPAPSS1/2 cells were seeded into the wells of 12-well plates and cultured in 1 ml of supplemented DMEM. Forty-eight hours later, culture medium was replaced with 1 ml of Opti-MEM I Reduced Serum Medium (Life Technologies). Then, 200 $\mu$l was added of a premixed complex of 4 $\mu$l Lipofectamine 2000 (Life Technologies) and plasmid DNA consisting of selected combinations of the following: 1500 ng of FXRE-Luc or a UGT2B4-Luc reporter plasmid, 150 ng pGL3-Promoter (Promega), 50 ng pcDNA3.1 (Life Technologies), 50 ng FXR expression plasmid (Origene), 1 ng pRL-SV40 (Promega), and sufficient pBluescript II KS$^+$ (Agilent Technologies) to keep the total amount of DNA constant among samples. Six or 24 hours later, the transfection medium was replaced with fresh supplemented DMEM alone or containing 0.1% dimethylsulfoxide, 10 $\mu$M 3-(2,6-dichlorophenyl)-4-(3′-carboxy-2-chlorostilben-4-yl)oxymethyl-5-isopropylisoxazole (GW4064), or 100 $\mu$M chenodeoxycholic acid. The cells were harvested the next day for measurement of firefly and *Renilla* luciferase activities using the Dual Luciferase Reporter Assay System and a GloMax Luminometer (Promega). Transfection data from the shNT and shPAPSS1/2 cell lines were normalized and analyzed as previously described (Barrett et al., 2013).

**RNA Interference.** shNT and shPAPSS1/2 cells were cultured as described previously. Forty-eight hours after seeding, culture medium was replaced with 1 ml of Opti-MEM I Reduced Serum Medium (Life Technologies). Then, 200 $\mu$l was added of a premixed complex of 4 $\mu$l Lipofectamine 2000, plasmid DNA, and small interfering RNA (siRNA) consisting of selected combinations of the following: 10 pmol FXR siRNA or nontargeting siRNA (ON-TARGET*plus* SMART pools, Thermo Scientific, Waltham, MA), 1450 ng FXRE-Luc or (−1991:13)-UGT2B4-Luc, 150 ng pGL3-Promoter (Promega), 1 ng pRL-SV40 (Promega), and sufficient pBluescript II KS$^+$ (Agilent Technologies) to keep the total amount of nucleic acid constant among samples. The following day, transfection medium was replaced with 1 ml of fresh supplemented DMEM containing 0.1% dimethylsulfoxide or 10 $\mu$M GW4064. Forty-eight hours post-transfection, cells were harvested for measurement of firefly and *Renilla* luciferase activity.

**UGT2B4 mRNA Synthesis and Stability.** UGT2B4 mRNA synthesis and stability in shNT and shPAPSS1/2 cells were assessed by pulse-chase analysis, using the Click-iT Nascent RNA Capture Kit essentially according to the manufacturer's instructions (Life Technologies). shNT and shPAPSS1/2 cells were incubated with DMEM containing the uridine analog ethynyl uridine (EU) (0.5 mM) for 1 hour. A portion of the cells was then harvested and total RNA was isolated for estimation of mRNA synthesis. The remaining cells were then rinsed with Hanks' balanced salt solution and the medium was replaced with EU-free DMEM. Cells were then harvested during this chase period at time points ranging from 2 to 10 hours after replacing the medium, and total RNA was isolated. Newly synthesized EU-labeled RNA was biotinylated and then captured with streptavidin Dynabeads. cDNA was synthesized from the captured EU-labeled RNA and UGT2B4 mRNA levels were measured by qRT-PCR. For estimation of UGT2B4 half-life, the relative level of EU-labeled UGT2B4 mRNA at each chase time point was calculated relative to the amount at the first chase time point, and the slope of the ln(UGT2B4 mRNA) versus time plot was calculated. Assuming first-order decay kinetics, $t_{1/2} = 0.693/-$ slope.

**Statistical Analysis.** qRT-PCR and promoter transfection data were analyzed using Student's *t* test or one-way analysis of variance followed by the Neuman-Keuls multiple comparison test. $P < 0.05$ was considered statistically significant.

## Results

**UGT2B4 Expression in PAPSS1/2-Deficient HepG2 Cells.** Microarray analysis indicated that 2944 genes were significantly differentially expressed in shPAPSS1/2 cells compared with shNT cells. Supplemental Table 2 shows the microarray results for the differentially expressed genes with fold differences of 2 or greater. The microarray analysis found no significant difference in SULT2A1 mRNA levels between the cell lines; however, UGT2B4 mRNA levels were 23.8-fold higher in shPAPSS1/2 cells than in shNT cells. The only other significant differences in UGT mRNA levels that were observed in the shPAPSS1/2 relative to the shNT cells were (1) an 18.7-fold increase in a sequence described as UGT2B28 precursor; (2) a 6.95-fold increase in UGT2A1; and (3) a 1.31-fold decrease in UGT2A3. In agreement with the microarray data, the qRT-PCR and western blot analyses indicated no difference in SULT2A1 mRNA (Fig. 1A) or protein (Fig. 1B) content between the shPAPSS1/2 and shNT cells. Figure 2A shows that UGT2B4 mRNA content was ~41-fold (40.7 ± 22.7) higher in shPAPSS1/2 cells than in shNT cells, while Fig. 2B shows that the amount of UGT2B4 protein was also significantly increased in the shPAPSS1/2 cells.

**UGT2B4 Expression in SULT2A1-Deficient HepG2 Cells.** SULT2A1 is the only human SULT that catalyzes BA sulfonation (Comer et al., 1993) and along with UGT2B4 plays an important role in hepatic BA homeostasis (Pillot et al., 1993). To determine whether knocking down SULT2A1 specifically would recapitulate the effect of global sulfotransferase suppression on UGT2B4, UGT2B4 expression was assessed in a HepG2 clone stably expressing a SULT2A1-targeting short hairpin RNA (shSULT2A1, described previously) (Barrett et al., 2013). UGT2B4 mRNA content was ~7-fold (6.6 ± 6.1) higher in shSULT2A1 cells compared with control cells (shNT) (Fig. 3A), and UGT2B4 protein content was also significantly higher (Fig. 3B).

**Lack of a Role for FXR in PAPSS Knockdown-Mediated Upregulation of UGT2B4.** UGT2B4 is a known target gene of FXR (Barbier et al., 2003), and Barrett et al. (2013) previously found that FXR activation was ~2.5-fold higher in shPAPSS1/2 cells compared with control cells. To examine whether FXR activation plays a role in the significant upregulation of UGT2B4 expression in shPAPSS1/2 cells, a luciferase reporter plasmid containing ~2 Kb of the UGT2B4

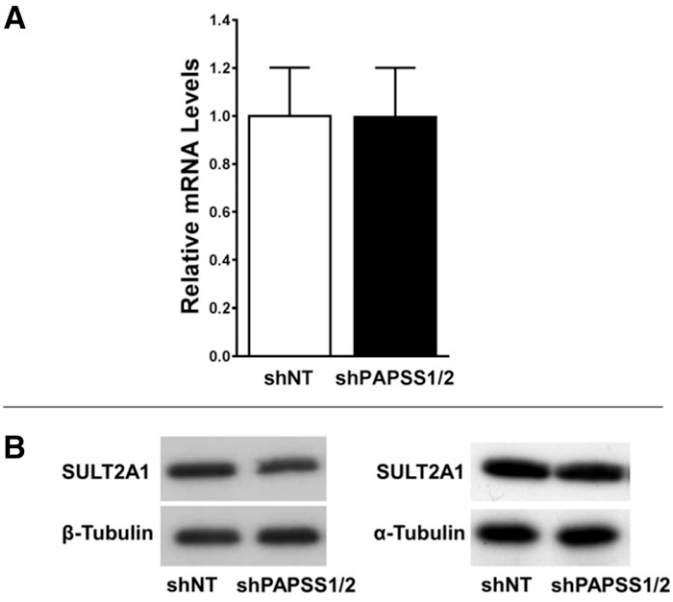


**Fig. 1.** Lack of effect of PAPSS1 and PAPSS2 knockdown on SULT2A1 expression in HepG2 cells. SULT2A1 mRNA (A) and protein (B) levels were measured in shNT and shPAPSS1/2 cells using TaqMan Gene Expression Assays and western blot analysis, respectively. (A) Each bar represents the mean mRNA level ± S.E.M. (relative to shNT cells) from three independent experiments. (B) Shows the immunoreactive bands from two independent experiments.

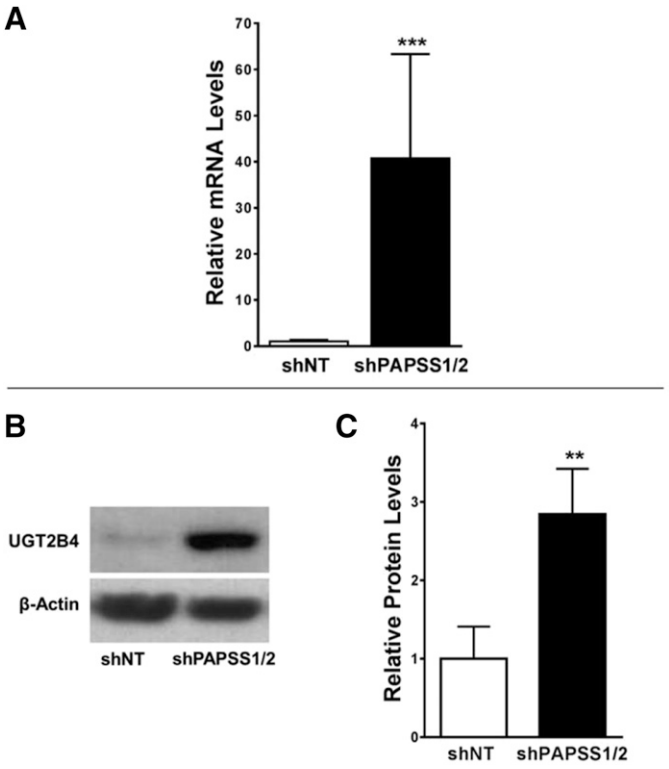


**Fig. 2.** PAPSS1 and PAPSS2 knockdown increases UGT2B4 expression in HepG2 cells. UGT2B4 mRNA (A) and protein (B, C) levels were measured in shNT and shPAPSS1/2 cells using TaqMan Gene Expression Assays and western blot analysis, respectively. (A) Each bar represents the mean mRNA level ± S.E.M. (relative to shNT cells) from four independent experiments. ***Significantly different from shNT, $P < 0.001$ using ratio paired $t$ test. (B) Shows the immunoreactive bands from one representative experiment; (C) shows the densitometrically quantified data from four independent experiments; each bar represents the mean ratio of UGT2B4/$\beta$-actin ± S.E.M. (relative to shNT cells). **Significantly different from shNT, $P < 0.01$ by paired $t$ test.

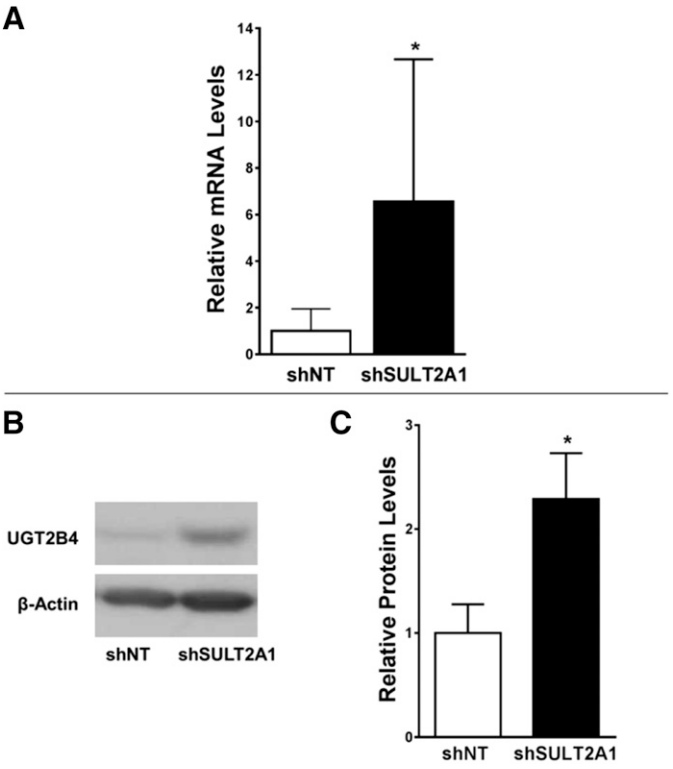


**Fig. 3.** SULT2A1 knockdown increases UGT2B4 expression in HepG2 cells. UGT2B4 mRNA (A) and protein (B, C) levels were measured in shNT and shSULT2A1 cells using TaqMan Gene Expression Assays and western blot analysis, respectively. (A) Each bar represents the mean relative mRNA level ± S.E.M. from three independent experiments. *Significantly different from shNT, $P < 0.05$ using ratio paired $t$ test. (B) Shows the immunoreactive bands from one representative experiment; (C) shows the densitometrically quantified data from three independent experiments; each bar represents the mean ratio of UGT2B4/$\beta$-actin ± S.E.M. (relative to shNT cells). *Significantly different from shNT, $P < 0.05$ by paired $t$ test.

5′-flanking region, which includes a FXRE at nucleotides −1193 to −1187 (Barbier et al., 2003), was transiently transfected into shNT and shPAPSS1/2 cells. Figure 4 shows that (−1991:+13)-UGT2B4-Luc activity is ~4-fold higher when transiently transfected into shPAPSS1/2 cells than when transfected into shNT cells. Treatment of transfected shPAPSS1/2 cells with a FXR agonist, GW4064 or chenodeoxycholic acid, for 24 hours increased UGT2B4 promoter activity ~4- and ~2-fold, respectively, compared with dimethylsulfoxide-treated shPAPSS1/2 cells (Fig. 5A). Also, cotransfection of shPAPSS1/2 cells with a FXR expression plasmid increased (−1991:+13)-UGT2B4-Luc activity ~4-fold compared with cotransfection with empty expression vector (Fig. 5B).

To determine whether UGT2B4 transcriptional activation in HepG2 cells with limited sulfonation capacity is mediated through FXR, FXR was knocked down in shPAPSS1/2 cells. Cotransfection of shPAPSS1/2 cells with a siRNA targeting FXR reduced GW4064-mediated activation of a FXR-responsive reporter plasmid (FXRE-Luc) by 97% (Fig. 6A), demonstrating effective knockdown of FXR; however, transient silencing of FXR did not diminish UGT2B4 reporter expression (Fig. 6B). Mutation of the UGT2B4 FXRE caused a reduction in luciferase activity of 22%, relative to UGT2B4 reporter containing the wild-type FXRE (Fig. 7). However, the mutated FXRE reporter activity in shPAPSS1/2 cells was still 3-fold higher than wild-type FXRE activity in shNT cells. These data indicate that FXR agonist treatment and FXR overexpression can activate the (−1991:+13)-UGT2B4-Luc reporter. However, FXR does not appear to be responsible for the upregulation of UGT2B4 that occurs in shPAPSS1/2 cells.

**Transcriptional Regulation of UGT2B4 in PAPSS1/2-Deficient HepG2 Cells.** To search for other possible *cis*-acting elements in the (−1991:+13)-UGT2B4-Luc reporter that could be responsible for conferring PAPSS1/2 deficiency-mediated UGT2B4 upregulation, a series of luciferase reporter plasmids containing UGT2B4 promoter fragments ranging in size from 1661 to 126 nucleotides was evaluated in shPAPSS1/2 and shNT cells (Fig. 8). The pattern of activity for all five constructs was the same in both cell lines, although the luciferase activity of each reporter was ~3-fold higher in shPAPSS1/2 cells than in shNT cells. Deletion of the FXRE, which resides in the 529 nucleotide sequence upstream of the (−1119:+13) fragment, did not reduce promoter activity, but rather increased activity. In fact, activity of (−1119:+13)-UGT2B4-Luc was significantly higher compared with all other constructs in shNT and shPAPSS1/2 cells. These data do not clearly implicate any region for the upregulation of UGT2B4 expression in shPAPSS1/2 cells, but suggest that activity may be conferred within the proximal 112 nucleotides.

To evaluate whether regions that contribute to UGT2B4 upregulation in shPAPSS1/2 cells are located farther upstream than 2 Kb, we examined up to ~16Kb of the 5′-flanking region of the UGT2B4 gene. Each successive upstream fragment was ~2Kb in size and all upstream fragments were ligated into (−112:+13)-UGT2B4-Luc as a common core promoter. Figure 9 shows the luciferase activities after the reporter series was transiently transfected into shPAPSS1/2 or shNT cells. For analysis of these data, luciferase activities were normalized to the activity of the core promoter reporter (−112:+13)-UGT2B4-Luc within each cell line, in

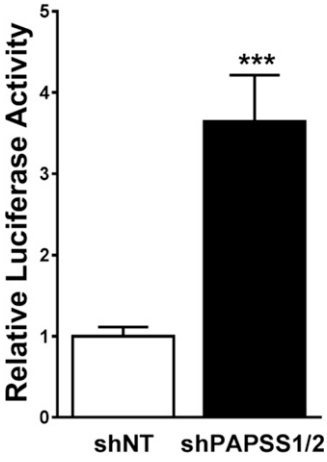


**Fig. 4.** UGT2B4 promoter activity is greater in shPAPSS1/2 than shNT HepG2 cells. shNT and shPAPSS1/2 cells were transfected with a luciferase reporter construct containing 1991 nucleotides of the 5′-flanking region of the UGT2B4 gene. Forty-eight hours after transfection, cells were harvested for measurement of luciferase activities. Each bar represents the mean ± S.D. normalized (firefly/*Renilla*) luciferase activity relative to the activity that was measured for the shNT cells ($n$ = 9 wells per group, derived from combining data from three independent experiments with triplicate transfection). ***Significantly different from shNT, $P < 0.001$ by unpaired $t$ test.

order to eliminate any contribution of the (−112:+13) fragment to differences between cell lines. When the data were analyzed in this manner, most constructs showed little or no difference in activity between the shNT and shPAPSS1/2 cell lines. The exception was (−12072:−10037)(−112:+13)-UGT2B4-Luc, which showed ~2-fold higher activity in shPAPSS1/2 cells than in shNT cells. The activity of this construct in shNT cells was also higher than that of other constructs containing more proximal UGT2B4 5′-flanking regions.

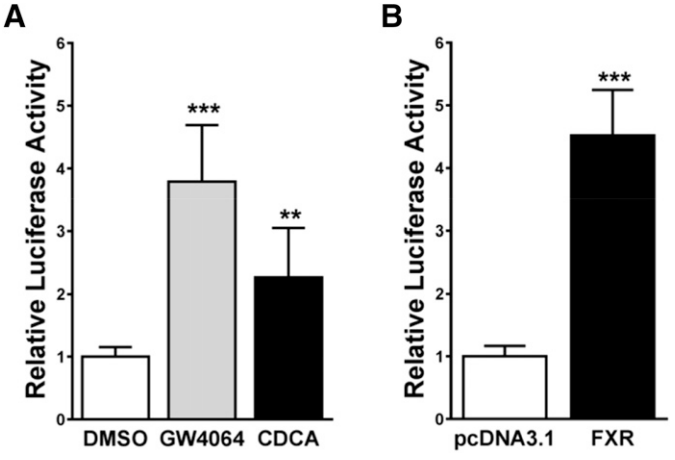


**Fig. 5.** UGT2B4 promoter response to FXR agonists and FXR overexpression in shPAPSS1/2 cells. (A) shPAPSS1/2 cells were transfected with a reporter construct containing 1991 nucleotides of the 5′-flanking region of the UGT2B4 gene. Twenty-four hours after transfection, cells were treated with 0.1% dimethylsulfoxide (DMSO), 10 $\mu$M GW4064, or 100 $\mu$M chenodeoxycholic acid (CDCA). (B) shPAPSS1/2 cells were cotransfected with (−1991:+13)-UGT2B4-Luc and FXR expression plasmid or the empty expression vector, pcDNA3.1. Forty-eight hours after transfection, cells were harvested and luciferase activities were measured. Each bar represents the mean ± S.D. normalized (firefly/*Renilla*) luciferase activity relative to the activity measured in DMSO-treated or pcDNA3.1-transfected cells ($n$ = 6 wells per group, derived from combining data from two independent experiments with triplicate transfection). **Significantly different from DMSO, $P < 0.01$; ***Significantly different from DMSO or pcDNA3.1, $P < 0.001$ by one-way analysis of variance and Neuman-Keuls test (A) or unpaired $t$ test (B).

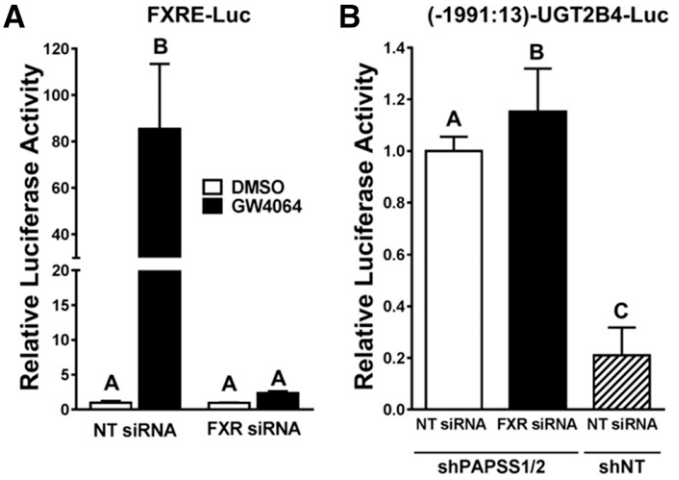


**Fig. 6.** Effect of knocking down FXR on UGT2B4 promoter activity in shPAPSS1/2 cells. (A) shPAPSS1/2 cells were transfected with a FXR-responsive reporter plasmid. Half of the cells were cotransfected with nontargeting siRNA, the other half with siRNA targeting FXR. Twenty-four hours after transfection cells were treated with 0.1% dimethylsulfoxide (DMSO) or 10 $\mu$M GW4064. (B) shPAPSS1/2 cells were transfected with a reporter construct containing 1991 nucleotides of the 5′-flanking region of the UGT2B4 gene; designated (−1991:+13)-UGT2B4-Luc. Half of the cells were cotransfected with nontargeting siRNA, the other half with FXR siRNA. Twenty-four hours after transfection, all cells were treated with 0.1% DMSO. Forty-eight hours after transfection, cells were harvested and luciferase activities were measured. Each bar represents the mean ± S.D. normalized (firefly/*Renilla*) luciferase activity ($n$ = 6 wells per group, derived from combining data from two independent experiments with triplicate transfection). In each panel, the mean value for the DMSO-treated, nontargeting (NT) siRNA-transfected shPAPSS1/2 cell group is defined as 1. Groups not sharing an upper case letter are significantly different from each other, $P < 0.05$ (by one-way analysis of variance and Neuman-Keuls test).

These data suggest that the (−12072:−10037) region of the UGT2B4 gene contains information that (1) positively regulates UGT2B4 transcription and (2) increases transcription to a greater extent in shPAPSS1/2 cells than in shNT cells.

Progressively refined deletion series were prepared to identify the region within the (−12072:10037) fragment that conferred enhanced UGT2B4 promoter activity in shNT and shPAPSS1/2 cells (Supplemental Figs. 2–4). The data show that the UGT2B4 information conferring increased luciferase activity is contained within the −10111:−10037 region. Supplemental Fig. 4 also shows that when (−10111:−10037) was shortened by 31 nucleotides, the promoter activity increased ~2-fold, suggesting the presence of a suppressive element between nucleotides −10111 and −10080.

LS mutagenesis analysis was then used to identify the sequence(s) that conferred enhanced transcriptional activity (Fig. 10). LS mutants LS1–LS9 were prepared to span nucleotides −10090 to −10037 using the (−10503:−10037)(−112:+13)-UGT2B4-Luc reporter as a template (schematic representation shown in Supplemental Fig. 1). The shPAPSS1/2 and shNT cells were transfected with mutants LS1–LS9, as well as with constructs (−10503:−10037)(−112:+13)-UGT2B4-Luc, (−10111:−10037) (−112:+13)-UGT2B4-Luc, and (−10080:−10037)(−112:+13)-UGT2B4-Luc for comparison. Reporter activity was normalized to the activity of the (−112:+13)-UGT2B4-Luc reporter within each cell line to exclude any contribution of the core promoter region to differences between the cell lines.

Replacing nucleotides −10090 to −10085 with a BamHI site (LS1 mutant) resulted in a significant increase in luciferase activity relative to constructs (−10503:−10037) and (−10111:−10037) (Fig. 10). The luciferase activity of LS1 was comparable to that of the (−10080:−10037)(−112:+13)-UGT2B4-Luc deletion construct, and activity

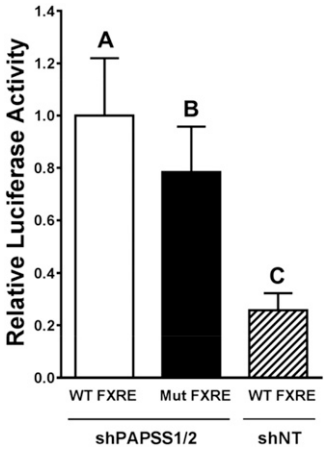


**Fig. 7.** Effect of mutating a FXRE on UGT2B4 promoter activity in shPAPSS1/2 cells. shPAPSS1/2 cells were transfected with a reporter construct containing 1991 nucleotides of the 5′-flanking region of the UGT2B4 gene, designated (−1991:+13)-UGT2B4-Luc, with either the wild-type FXRE (WT FXRE) or mutated FXRE (Mut FXRE). shNT cells were transfected with the reporter containing the WT FXRE. Forty-eight hours after transfection, cells were harvested and luciferase activities were measured. Each bar represents the mean ± S.D. of normalized (firefly/*Renilla*) luciferase measurements relative to the activity measured in WT FXRE–transfected shPAPSS1/2 cells ($n$ = 6 wells per group, derived from combining data from two independent experiments with triplicate transfection). Groups not sharing an upper case letter are significantly different from each other, $P < 0.05$ (by one-way analysis of variance and Neuman-Keuls test).

was ~2-fold higher in shPAPSS1/2 cells than in shNT cells. Promoter activity was reduced somewhat in mutants LS2–LS6 compared with constructs (−10503:−10037) and (−10111:−10037), and activity in LS2–LS6 was ~1.2- to 2-fold higher when transfected into shPAPSS1/2 cells compared with shNT cells. Disrupting any of the last 18 nucleotides of the (−10503:−10037) fragment (mutant LS7, LS8, or LS9) reduced luciferase activity to core promoter reporter levels. Therefore, these data identified two distal *cis*-regulatory regions in the 5′-flanking region of the UGT2B4 gene that negatively and positively regulated transcription: (1) between nucleotides −10090 and −10085 and (2) between nucleotides −10054 and −10037. Computational analysis was performed on nucleotides −10090 to −10037 to identify putative transcription factor binding sites (MatInspector software; Genomatrix, Inc., Cincinnati, OH) (Quandt et al., 1995; Cartharius et al., 2005). Supplemental Table 3 lists the matrix, description, strand, core and matrix similarity, sequence, and core sequence location in the LS mutants. Twenty-four of the 32 predicted binding sites are for homeodomain proteins, and several of these are located within the LS1 mutation that marked a suppressive element or within the LS7-9 mutations that indicated an enhancer(s). The LS2–LS6 mutations, which all partially reduced reporter expression, also contained predicted binding sites for homeodomain proteins, such as the POU class 2 homeobox 1 (OCT1) (in LS2 and LS3), which has been implicated in the regulation of UGT2B7 (Ishii et al., 2000). The LS2–LS6 region also contained sites for other transcription factors that could be expected to contribute to UGT2B4 transcription, such as the liver-enriched transcription factors, forkhead box factors (in LS3) and CCAAT/enhancer binding protein $\alpha$ (in LS3 and LS4), and the lipid-activated nuclear receptor peroxisome proliferator-activated receptor $\gamma$ (in LS4 and LS5).

**Regulation of UGT2B4 mRNA Synthesis and Stability in PAPSS1/2-Deficient HepG2 Cells.** To determine whether increased transcript stability contributes to the significant upregulation of UGT2B4 mRNA in HepG2 cells with diminished sulfonation capacity, we analyzed de novo mRNA synthesis and decay by pulse-chase analysis. Following EU pulse labeling, UGT2B4 mRNA synthesis was 15.6 ± 4.8-fold higher in shPAPSS1/2 cells than in shNT cells (mean ± S.E.M. of seven independent experiments). The decreases in EU-labeled mRNA levels during the chase period indicated that the half-life of UGT2B4 mRNA in shNT cells was 2.23 ± 0.35 hours, whereas the half-life in shPAPSS1/2 cells was 9.80 ± 4.34 (means ± S.E.M. of four experiments). Although the data were somewhat variable across multiple independent experiments, overall they suggest that the accumulation of UGT2B4 mRNA in shPAPSS1/2 cells is likely attributable to a combination of a higher de novo mRNA synthesis rate and longer half-life.

The 3′-UTR is known to regulate mRNA translation efficiency, stability, and localization (Guhaniyogi and Brewer, 2001). To determine whether the 3′-UTR of UGT2B4 influences mRNA levels in shPAPSS1/2 cells, we ligated the UGT2B4 3′-UTR region downstream from the Luc coding region and transfected this reporter or the empty vector into shPAPSS1/2 and shNT cells. Figure 11 shows that the UGT2B4 3′-UTR reduced luciferase activity more in shNT cells (31% reduction relative to empty vector) than in shPAPSS1/2 cells (21% reduction), indicating that the

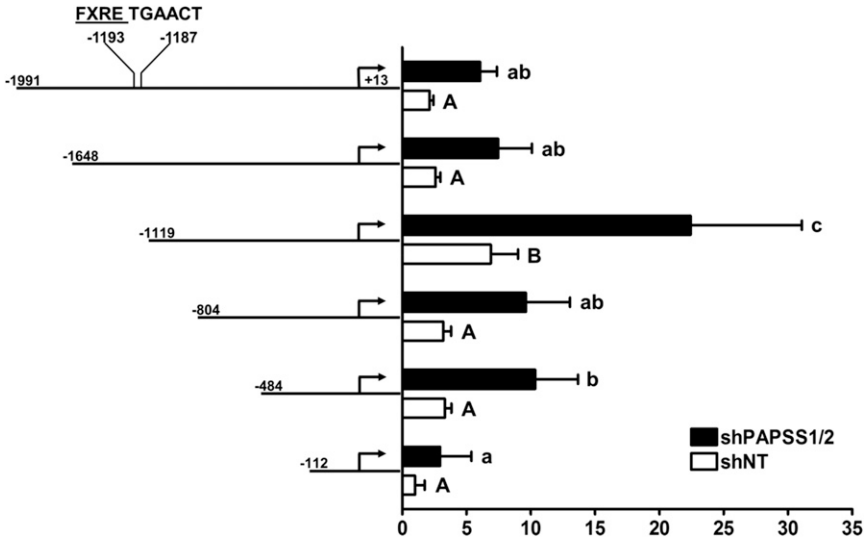


**Fig. 8.** Promoter activities of a nested deletion series of reporter plasmids constructed from (−1991:+13)-UGT2B4-Luc. shNT and shPAPSS1/2 cells were transfected with the indicated reporter plasmids. Forty-eight hours after transfection, cells were harvested for measurement of luciferase activities. Each bar represents the mean ± S.D. of normalized (firefly/*Renilla*) luciferase measurements relative to the activity measure in shNT cells transfected with (−112:+13)-UGT2B4-Luc ($n$ = 6 wells per group, derived from combining data from two independent experiments with triplicate transfection). For shNT cells, groups not sharing an upper case letter are significantly different from each other, $P < 0.05$. For shPAPSS1/2 cells, groups not sharing a lower case letter are significantly different from each other, $P < 0.05$ (by one-way analysis of variance and Neuman-Keuls test).

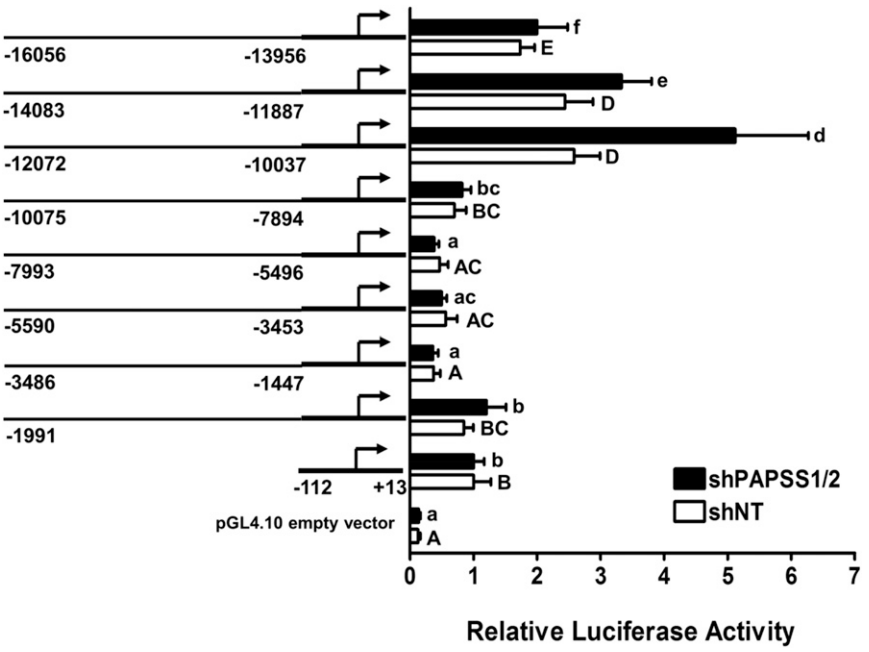


**Fig. 9.** Transient transfection analysis of the effects of upstream 5′-flanking regions of the UGT2B4 gene on promoter activity in shPAPSS1/2 cells and shNT cells. The indicated 5′-flanking regions of the UGT2B4 gene were ligated into the pGL4.10 plasmid upstream of nucleotides −112 to +13, which served as the common proximal promoter for all constructs. Reporter activities of (−1991:+13)-UGT2B4-Luc, used in previous experiments (labeled −1991), (−112:+13)-UGT2B4-Luc, and pGL4.10 empty vector are shown for comparison. shNT and shPAPSS1/2 cells were transfected with the reporters and 48 hours later were harvested for measurement of luciferase activities. Each bar represents the mean ± S.D. of normalized (firefly/*Renilla*) luciferase measurements relative to the activity measured in cells transfected with (−112:+13)-UGT2B4-Luc within each cell line ($n$ = 12 wells per group, derived from combining data from four independent experiments with triplicate transfection). For shNT cells, groups not sharing an upper case letter are significantly different from each other, $P < 0.05$. For shPAPSS1/2 cells, groups not sharing a lower case letter are significantly different from each other, $P < 0.05$ (by one-way analysis of variance and Neuman-Keuls test).

UGT2B4 3′-UTR exerted a stabilizing effect in the shPAPSS1/2 cells relative to the shNT cells. Taken together with the pulse-chase data, these results suggest that PAPSS knockdown increases the stability of UGT2B4 mRNA through a mechanism that is mediated through its 3′-UTR.

We performed a computational analysis of predicted micro-RNA binding sites in the 3′-UTR of human UGT2B4. To reduce false positives we used a consensus of 10 prediction algorithms available through miRWalk (Dweep et al., 2011). This analysis identified 23 micro-RNAs that were predicted by at least five algorithms to target UGT2B4 (Supplemental Table 4).

## Discussion

Dawson et al. (2006) and Barrett et al. (2013) previously reported that hyposulfatemic mice lacking the renal NaS1 transporter had increased hepatic Sult2a1 expression in an apparent attempt to compensate for reduced sulfonation capacity. Consistent with that interpretation, knockdown of the enzymes responsible for synthesis of PAPS (PAPSS1 and 2), the obligate cofactor for all sulfonation reactions, activated transfected Sult2a1 promoter constructs in HepG2 cells. Specific knockdown of SULT2A1 in HepG2 cells also caused activation of the mouse Sult2a1 promoter, suggesting that transcriptional activation of mouse Sult2a1 occurs specifically in response to

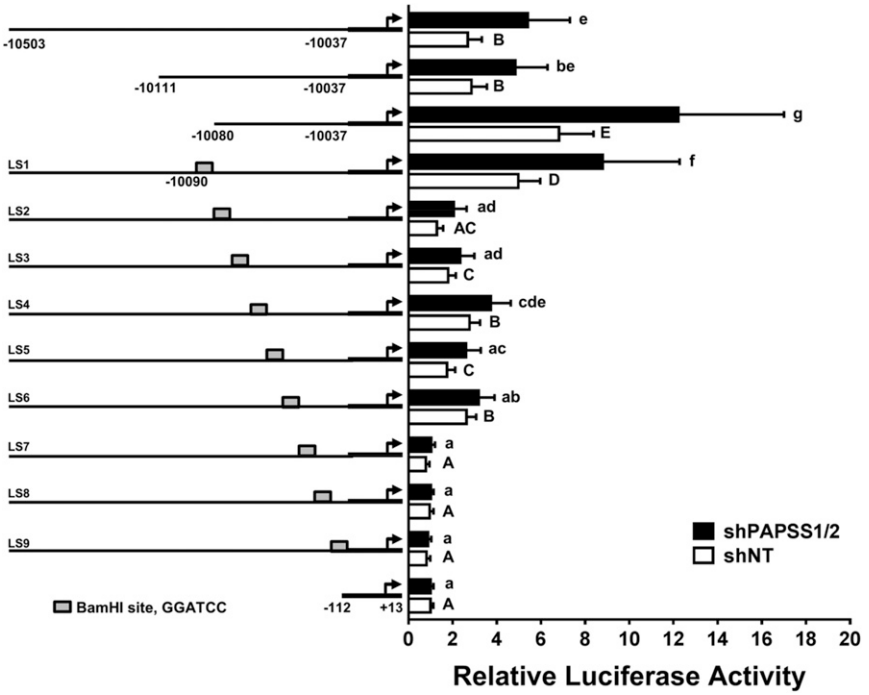


**Fig. 10.** Impact of LS mutagenesis on the activity of the (−10503:−10037)(−112:+13)-UGT2B4-Luc reporter. LS mutants and two deletion constructs were constructed from (−10503:−10037)(−112:+13)-UGT2B4-Luc. LS1–LS9 mutants span nucleotides −10090 to −10037. shNT and shPAPSS1/2 cells were transfected with the reporters as indicated. Forty-eight hours later, cells were harvested for measurement of luciferase activities. Each bar represents the mean ± S.D. of normalized (firefly/*Renilla*) luciferase measurements relative to the activity measured in cells transfected with (−112:+13)-UGT2B4-Luc within each cell line ($n$ = 12 wells per group, derived from combining data from four independent experiments with triplicate transfection). For shNT cells, groups not sharing an upper case letter are significantly different from each other, $P < 0.05$. For shPAPSS1/2 cells, groups not sharing a lower case letter are significantly different from each other, $P < 0.05$ (by one-way analysis of variance and Neuman-Keuls test).

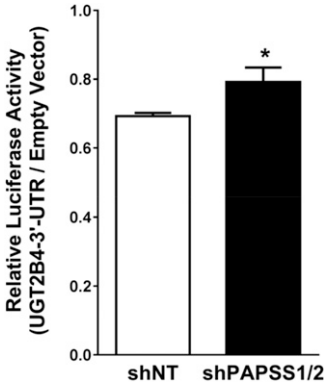


**Fig. 11.** Impact of UGT2B4 3′-UTR on luciferase activity in shNT and shPAPSS1/2 cells. The UGT2B4 3′-UTR was ligated downstream from the Luc gene in the pmirGLO luciferase reporter vector. UGT2B4-3′-UTR/pmirGLO or empty vector was transfected into shNT or shPAPSS1/2 cells, and 48 hours later cells were harvested for measurement of luciferase activities. Each bar represents the mean ratio ± S.E.M. ($n$ = 8 independent experiments) of normalized (firefly/*Renilla*) UGT2B4 3′-UTR luciferase measurements relative to the activity measured in cells transfected with the empty vector within each cell line. *Significantly different from shNT, $P < 0.05$ by paired $t$ test.

loss of SULT2A1-mediated metabolism of some endogenous molecule. However, a major species difference between mice and humans was observed because PAPSS1/2 knockdown did not cause upregulation of endogenous SULT2A1 in HepG2 cells but instead caused marked upregulation of UGT2B4. These results demonstrate a physiologic linkage between SULT2A1 and UGT2B4 regulation in humans.

The concept of overlap between SULTs and UGTs is well established since these enzyme systems share many substrates and mechanisms of regulation. Sulfonation is generally considered to be a high-affinity, low-capacity reaction while glucuronidation is a low-affinity, high-capacity reaction (Parkinson et al., 2013). As substrate concentrations increase and SULTs become saturated or PAPS is depleted, glucuronidation increases (Morris and Pang, 1987; Zamek-Gliszczynski et al., 2006).

Redundancy between conjugation pathways occurs as a protective mechanism during cholestasis. In healthy adults, the biliary pathway is the preferred route for BA excretion, and sulfonation is the predominant detoxification pathway (Radominska et al., 1990; Comer et al., 1993). However, under cholestatic conditions serum and urinary BA sulfonates and glucuronides increase (Fröhling and Stiehl, 1976; van Berge Henegouwen et al., 1976; Stiehl et al., 1980; Meng et al., 1997). The shift to the urinary pathway for BA excretion acts as a defense mechanism to protect the hepatocytes from the harmful effects of BA accumulation. Increased glucuronidation appears to act as a back-up mechanism to detoxify excess BAs when the sulfonation pathway becomes saturated.

A functional relationship between SULT2A1 and UGT2B4 in BA detoxification has been established by their roles in metabolism of the toxic secondary BA lithocholic acid (LCA) (Miyal et al., 1975). SULT2A1 has high activity toward LCA, and catalyzes this reaction with an apparent Km of ~1.5 $\mu$M (Radominska et al., 1990). However, SULT2A1 has relatively low activity toward the 6$\alpha$-hydroxylated metabolite of LCA, hyodeoxycholic acid (HDCA) (Radominska et al., 1990). By contrast, UGT2B4 has little activity toward LCA but efficiently glucuronidates HDCA (Radomińska-Pyrek et al., 1987; Pillot et al., 1993) with a Km of ~25 $\mu$M (Barre et al., 2007). The available evidence suggests that LCA 6$\alpha$-hydroxylation is catalyzed mainly by CYP3A4 with a Km of ~45 $\mu$M (Araya and Wikvall, 1999; Deo and Bandiera, 2009). Therefore, under normal physiologic conditions, LCA is mainly detoxified by SULT2A1-mediated sulfonation, and 6$\alpha$-hydroxlyated BA levels remain low (Summerfield et al., 1976; Shoda et al., 1990; Wietholtz et al., 1996). Elevation of LCA levels results in increased HDCA formation by CYP3A4-mediated 6$\alpha$-hydroxylation, a reaction that is facilitated by LCA-mediated activation of PXR (Staudinger et al., 2001; Stedman et al., 2004). The HDCA that is formed is then glucuronidated by UGT2B4.

The BA-sensing nuclear receptor FXR controls expression of several genes that are involved in BA synthesis, transport, and metabolism (Makishima et al., 1999; Wang et al., 1999; Goodwin et al., 2000; Sinal et al., 2000; Song et al., 2001; Barbier et al., 2003; Landrier et al., 2006; Kim et al., 2007), and Barrett et al. (2013) previously reported higher FXR activity in PAPSS1/2-deficient HepG2 cells than in control cells. Additionally, Barrett et al. (2013) attributed activation of murine Sult2a1 in shPAPSS1/2 cells to a FXR-mediated mechanism. UGT2B4 has been reported to contain a functional FXRE, although this FXRE is atypical in that it binds FXR as a monomer (Barbier et al., 2003). We confirmed the FXR responsiveness of the UGT2B4 promoter by showing that treatment with a FXR agonist or FXR overexpression activated UGT2B4 promoter activity. However, activation through the reported FXRE could not explain the marked upregulation of UGT2B4 that occurred in shPAPSS1/2 cells, since neither knocking down FXR nor mutating or deleting the FXRE reduced UGT2B4 promoter activity in shPAPSS1/2 to the level that was observed in control cells.

Our microarray analysis did not indicate that PAPSS knockdown caused widespread regulation of genes that are involved in BA homeostasis, although CYP7A1 mRNA content was 2.2-fold higher and ATP-binding cassette, subfamily C, member 2 mRNA content was 1.9-fold lower in the PAPSS1/2 knockdown cells. This suggests that UGT2B4 upregulation by sulfonation deficiency is not part of the paradigmatic mechanism for controlling BA homeostasis but is rather part of a more restricted portion of BA regulation that specifically controls conjugation as a detoxifying mechanism. In this regard, several genes involved in BA conjugation were significantly regulated by PAPSS knockdown (Supplemental Table 2). For example, UGT2A1, which also catalyzes BA conjugation (Perreault et al., 2013), was upregulated 6.95-fold by PAPSS knockdown. Also, CYP3A5 and CYP3A7 were upregulated (~3-fold). As noted previously, CYP3A-mediated catalysis is necessary to convert the BAs that are good substrates for sulfonation into the 6$\alpha$-hydroxylated metabolites that are the preferred substrates for glucuronidation. Altogether, these gene expression changes suggest that loss of sulfonation causes a shift toward a phenotype that favors BA glucuronidation in an attempt to prevent hepatotoxicity.

Evaluation of UGT2B4 5′-flanking sequences upstream of the reported FXRE identified a region approximately 10–12 Kb upstream of the transcription start site that augmented UGT2B4 promoter activity in shPAPSS1/2 cells. Deletion and LS mutagenesis analyses identified two closely localized regions from nucleotides −10090 to −10085 and nucleotides −10054 to −10037 that had opposing effects on UGT2B4 transcription. The more upstream region negatively regulated UGT2B4 transcription while the more downstream region positively regulated transcription. Computational analysis identified a large number of putative homeodomain binding sites within these regions (Supplemental Table 3). We hypothesize that these two regions function together as a composite regulatory module and that at least some of the proteins that interact with this module are sensitive to the sulfonation status of the cell. Detailed analysis is required to identify the specific regulatory proteins that interact with this module and to determine how sulfonation deficiency alters the activities of these factors.

An increase in steady-state mRNA level could occur through an increase in the rate of mRNA synthesis, a decrease in the rate of degradation, or a combination of both. Pulse-chase analysis confirmed that increased mRNA synthesis was an important determinant of increased UGT2B4 expression in shPAPSS1/2 cells but also indicated that the half-life of UGT2B4 mRNA was longer in shPAPSS1/2 cells than it was in control cells. This increase in UGT2B4 mRNA stability is likely mediated through the 3′-UTR since reporter assays demonstrated that the suppressive effect of the UGT2B4 3′-UTR was less in shPAPSS1/2 cells than in control cells. 3′-UTRs frequently contain regulatory sequences that can be bound by *trans*-acting factors, such as RNA-binding proteins and micro-RNAs, which positively or negatively modulate mRNA stability, localization, or translation efficiency (Guhaniyogi and Brewer, 2001; Mata et al., 2005; Wu and Brewer, 2012). Little is known about the regulation of UGT2B4 by micro-RNAs. Of the miRNAs that were computationally predicted to target the UGT2B4 3′-UTR (Supplemental Table 4), at least five (miR-629, miR-101, miR-203, miR-223, and miR-216b) have been reported to be expressed in HepG2 cells and regulate such processes as cell proliferation, DNA methylation, hepatocyte nuclear factor 4$\alpha$ activity, cytochrome P450 activities, multidrug resistance, and lipoprotein cholesterol uptake (Hatziapostolou et al., 2011; Huang et al., 2012; Wang et al., 2013; Wei et al., 2013a,b; Yang et al., 2013; Takahashi et al., 2014; Liu et al., 2015). Some evidence involving single nucleotide polymorphisms that have been identified in the 3′-UTRs of UGTs suggests that post-transcriptional regulation might contribute to interindividual variability in glucuronidation. For example, single nucleotide polymorphism rs3100 of the UGT2B15 3′-UTR increased expression from a luciferase 3′-UTR reporter, suggesting that this single nucleotide polymorphism might increase UGT2B15 expression and activity (Sun et al., 2011).

In summary, knocking down sulfonation capacity in a human liver cell model increases UGT2B4 expression by increasing transcriptional activation and enhancing mRNA stability. The combined effects of increasing both transcription and mRNA stability would result in a greater accumulation of intracellular UGT2B4 mRNA that is available for translation. The upregulation of this important BA-conjugating UGT may occur as a compensatory mechanism in response to the loss of sulfotransferase activity to prevent the buildup of BAs. Further studies are required to elucidate the specific activating and suppressive elements within the 5′-flanking region of the UGT2B4 gene and the 3′-UTR of the UGT2B4 transcript, as well as their respective binding factors, that operate as low sulfate sensors in the upregulation of UGT2B4.

### Authorship Contributions

*Participated in research design*: Barrett, Kocarek, Dombkowski, Runge-Morris.

*Conducted experiments*: Barrett, Fang, Cukovic.

*Performed data analysis*: Barrett, Dombkowski, Kocarek.

*Wrote or contributed to the writing of the manuscript*: Barrett, Kocarek, Runge-Morris.

### References


Araya Z and Wikvall K (1999) 6α-hydroxylation of taurochenodeoxycholic acid and lithocholic acid by CYP3A4 in human liver microsomes. *Biochim Biophys Acta* **1438:**47–54.

Barbier O, Torra IP, Sirvent A, Claudel T, Blanquart C, Duran-Sandoval D, Kuipers F, Kosykh V, Fruchart JC, and Staels B (2003) FXR induces the UGT2B4 enzyme in hepatocytes: a potential mechanism of negative feedback control of FXR activity. *Gastroenterology* **124:**1926–1940.

Barre L, Fournel-Gigleux S, Finel M, Netter P, Magdalou J, and Ouzzine M (2007) Substrate specificity of the human UDP-glucuronosyltransferase UGT2B4 and UGT2B7. Identification of a critical aromatic amino acid residue at position 33. *FEBS J* **274:**1256–1264.

Barrett KG, Fang H, Gargano MD, Markovich D, Kocarek TA, and Runge-Morris M (2013) Regulation of murine hepatic hydroxysteroid sulfotransferase expression in hyposulfatemic mice and in a cell model of 3′-phosphoadenosine-5′-phosphosulfate deficiency. *Drug Metab Dispos* **41:**1505–1513.

Cartharius K, Frech K, Grote K, Klocke B, Haltmeier M, Klingenhoff A, Frisch M, Bayerlein M, and Werner T (2005) MatInspector and beyond: promoter analysis based on transcription factor binding sites. *Bioinformatics* **21:**2933–2942.

Comer KA, Falany JL, and Falany CN (1993) Cloning and expression of human liver dehydroepiandrosterone sulphotransferase. *Biochem J* **289:**233–240.

Court MH, Zhang X, Ding X, Yee KK, Hesse LM, and Finel M (2012) Quantitative distribution of mRNAs encoding the 19 human UDP-glucuronosyltransferase enzymes in 26 adult and 3 fetal tissues. *Xenobiotica* **42:**266–277.

Dawson PA, Beck L, and Markovich D (2003) Hyposulfatemia, growth retardation, reduced fertility, and seizures in mice lacking a functional NaSi-1 gene. *Proc Natl Acad Sci USA* **100:** 13704–13709.

Dawson PA, Gardiner B, Grimmond S, and Markovich D (2006) Transcriptional profile reveals altered hepatic lipid and cholesterol metabolism in hyposulfatemic NaS1 null mice. *Physiol Genomics* **26:**116–124.

Deo AK and Bandiera SM (2009) 3-ketocholanoic acid is the major in vitro human hepatic microsomal metabolite of lithocholic acid. *Drug Metab Dispos* **37:**1938–1947.

Dweep H, Sticht C, Pandey P, and Gretz N (2011) miRWalk—database: prediction of possible miRNA binding sites by "walking" the genes of three genomes. *J Biomed Inform* **44:**839–847.

Fröhling W and Stiehl A (1976) Bile salt glucuronides: identification and quantitative analysis in the urine of patients with cholestasis. *Eur J Clin Invest* **6:**67–74.

Goodwin B, Jones SA, Price RR, Watson MA, McKee DD, Moore LB, Galardi C, Wilson JG, Lewis MC, and Roth ME, et al. (2000) A regulatory cascade of the nuclear receptors FXR, SHP-1, and LRH-1 represses bile acid biosynthesis. *Mol Cell* **6:**517–526.

Guhaniyogi J and Brewer G (2001) Regulation of mRNA stability in mammalian cells. *Gene* **265:** 11–23.

Gustin K and Burk RD (2000) PCR-directed linker scanning mutagenesis. *Methods Mol Biol* **130:** 85–90.

Hatziapostolou M, Polytarchou C, Aggelidou E, Drakaki A, Poultsides GA, Jaeger SA, Ogata H, Karin M, Struhl K, and Hadzopoulou-Cladaras M, et al. (2011) An HNF4α-miRNA inflammatory feedback circuit regulates hepatocellular oncogenesis. *Cell* **147:**1233–1247.

Huang Y, Chen HC, Chiang CW, Yeh CT, Chen SJ, and Chou CK (2012) Identification of a two-layer regulatory network of proliferation-related microRNAs in hepatoma cells. *Nucleic Acids Res* **40:**10478–10493.

Ishii Y, Hansen AJ, and Mackenzie PI (2000) Octamer transcription factor-1 enhances hepatic nuclear factor-1alpha-mediated activation of the human UDP glucuronosyltransferase 2B7 promoter. *Mol Pharmacol* **57:**940–947.

Izukawa T, Nakajima M, Fujiwara R, Yamanaka H, Fukami T, Takamiya M, Aoki Y, Ikushiro S, Sakaki T, and Yokoi T (2009) Quantitative analysis of UDP-glucuronosyltransferase (UGT) 1A and UGT2B expression levels in human livers. *Drug Metab Dispos* **37:**1759–1768.

Kim I, Ahn SH, Inagaki T, Choi M, Ito S, Guo GL, Kliewer SA, and Gonzalez FJ (2007) Differential regulation of bile acid homeostasis by the farnesoid X receptor in liver and intestine. *J Lipid Res* **48:**2664–2672.

Klaassen CD and Boles JW (1997) Sulfation and sulfotransferases 5: the importance of 3′-phosphoadenosine 5′-phosphosulfate (PAPS) in the regulation of sulfation. *FASEB J* **11:**404–418.

Kocarek TA and Mercer-Haines NA (2002) Squalestatin 1-inducible expression of rat CYP2B: evidence that an endogenous isoprenoid is an activator of the constitutive androstane receptor. *Mol Pharmacol* **62:**1177–1186.

Landrier JF, Eloranta JJ, Vavricka SR, and Kullak-Ublick GA (2006) The nuclear receptor for bile acids, FXR, transactivates human organic solute transporter-α and -β genes. *Am J Physiol Gastrointest Liver Physiol* **290:**G476–G485.

Liu FY, Zhou SJ, Deng YL, Zhang ZY, Zhang EL, Wu ZB, Huang ZY, and Chen XP (2015) MiR-216b is involved in pathogenesis and progression of hepatocellular carcinoma through HBx-miR-216b-IGF2BP2 signaling pathway. *Cell Death.Dis* **6:**e1670.

Makishima M, Okamoto AY, Repa JJ, Tu H, Learned RM, Luk A, Hull MV, Lustig KD, Mangelsdorf DJ, and Shan B (1999) Identification of a nuclear receptor for bile acids. *Science* **284:**1362–1365.

Mata J, Marguerat S, and Bähler J (2005) Post-transcriptional control of gene expression: a genome-wide perspective. *Trends Biochem Sci* **30:**506–514.

Meng LJ, Reyes H, Axelson M, Palma J, Hernandez I, Ribalta J, and Sjövall J (1997) Progesterone metabolites and bile acids in serum of patients with intrahepatic cholestasis of pregnancy: effect of ursodeoxycholic acid therapy. *Hepatology* **26:**1573–1579.

Miyal K, Mayr WW, and Richardson AL (1975) Acute cholestasis induced by lithocholic acid in the rat. A freeze-fracture replica and thin section study. *Lab Invest* **32:**527–535.

Morris ME and Pang KS (1987) Competition between two enzymes for substrate removal in liver: modulating effects due to substrate recruitment of hepatocyte activity. *J Pharmacokinet Biopharm* **15:**473–496.

Ohno S and Nakajin S (2009) Determination of mRNA expression of human UDP-glucuronosyltransferases and application for localization in various human tissues by real-time reverse transcriptase-polymerase chain reaction. *Drug Metab Dispos* **37:**32–40.

Parkinson A, Ogilvie B, Buckley D, Kazmi F, Czerwinski M, and Parkinson O (2013) Biotransformation of Xenobiotics, in *Casarett & Doull's Toxicology: The Basic Science of Poisons* (Klaassen CD ed) pp 185–368, McGraw Hill Education, New York.

Perreault M, Gauthier-Landry L, Trottier J, Verreault M, Caron P, Finel M, and Barbier O (2013) The Human UDP-glucuronosyltransferase UGT2A1 and UGT2A2 enzymes are highly active in bile acid glucuronidation. *Drug Metab Dispos* **41:**1616–1620.

Pillot T, Ouzzine M, Fournel-Gigleux S, Lafaurie C, Radominska A, Burchell B, Siest G, and Magdalou J (1993) Glucuronidation of hyodeoxycholic acid in human liver. Evidence for a selective role of UDP-glucuronosyltransferase 2B4. *J Biol Chem* **268:**25636–25642.

Quandt K, Frech K, Karas H, Wingender E, and Werner T (1995) MatInd and MatInspector: new fast and versatile tools for detection of consensus matches in nucleotide sequence data. *Nucleic Acids Res* **23:**4878–4884.

Radominska A, Comer KA, Zimniak P, Falany J, Iscan M, and Falany CN (1990) Human liver steroid sulphotransferase sulphates bile acids. *Biochem J* **272:**597–604.

Radomińska-Pyrek A, Zimniak P, Irshaid YM, Lester R, Tephly TR, and St Pyrek J (1987) Glucuronidation of 6 alpha-hydroxy bile acids by human liver microsomes. *J Clin Invest* **80:**234–241.

Rondini EA, Fang H, Runge-Morris M, and Kocarek TA (2014) Regulation of human cytosolic sulfotransferases 1C2 and 1C3 by nuclear signaling pathways in LS180 colorectal adenocarcinoma cells. *Drug Metab Dispos* **42:**361–368.

Shoda J, Tanaka N, Osuga T, Matsuura K, and Miyazaki H (1990) Altered bile acid metabolism in liver disease: concurrent occurrence of C-1 and C-6 hydroxylated bile acid metabolites and their preferential excretion into urine. *J Lipid Res* **31:**249–259.

Sinal CJ, Tohkin M, Miyata M, Ward JM, Lambert G, and Gonzalez FJ (2000) Targeted disruption of the nuclear receptor FXR/BAR impairs bile acid and lipid homeostasis. *Cell* **102:** 731–744.

Song CS, Echchgadda I, Baek BS, Ahn SC, Oh T, Roy AK, and Chatterjee B (2001) Dehydroepiandrosterone sulfotransferase gene induction by bile acid activated farnesoid X receptor. *J Biol Chem* **276:**42549–42556.

Staudinger JL, Goodwin B, Jones SA, Hawkins-Brown D, MacKenzie KI, LaTour A, Liu Y, Klaassen CD, Brown KK, and Reinhard J, et al. (2001) The nuclear receptor PXR is a lithocholic acid sensor that protects against liver toxicity. *Proc Natl Acad Sci USA* **98:**3369–3374.

Stedman C, Robertson G, Coulter S, and Liddle C (2004) Feed-forward regulation of bile acid detoxification by CYP3A4: studies in humanized transgenic mice. *J Biol Chem* **279:** 11336–11343.

Stiehl A, Becker M, Czygan P, Fröhling W, Kommerell B, Rotthauwe HW, and Senn M (1980) Bile acids and their sulphated and glucuronidated derivatives in bile, plasma, and urine of children with intrahepatic cholestasis: effects of phenobarbital treatment. *Eur J Clin Invest* **10:** 307–316.

Summerfield JA, Billing BH, and Shackleton CH (1976) Identification of bile acids in the serum and urine in cholestasis. Evidence for 6alpha-hydroxylation of bile acids in man. *Biochem J* **154:**507–516.

Sun C, Southard C, Olopade OI, and Di Rienzo A (2011) Differential allelic expression of c.1568C > A at UGT2B15 is due to variation in a novel *cis*-regulatory element in the 3′UTR. *Gene* **481:**24–28.

Takahashi K, Oda Y, Toyoda Y, Fukami T, Yokoi T, and Nakajima M (2014) Regulation of cytochrome b5 expression by miR-223 in human liver: effects on cytochrome P450 activities. *Pharm Res* **31:**780–794.

Takikawa H, Beppu T, Seyama Y, and Sugimoto T (1986) Glucuronidated and sulfated bile acids in serum of patients with acute hepatitis. *Dig Dis Sci* **31:**487–491.

van Berge Henegouwen GP, Brandt KH, Eyssen H, and Parmentier G (1976) Sulphated and unsulphated bile acids in serum, bile, and urine of patients with cholestasis. *Gut* **17:**861–869.

Wang H, Chen J, Hollister K, Sowers LC, and Forman BM (1999) Endogenous bile acids are ligands for the nuclear receptor FXR/BAR. *Mol Cell* **3:**543–553.

Wang L, Jia XJ, Jiang HJ, Du Y, Yang F, Si SY, and Hong B (2013) MicroRNAs 185, 96, and 223 repress selective high-density lipoprotein cholesterol uptake through posttranscriptional inhibition. *Mol Cell Biol* **33:**1956–1964.

Wei W, Wanjun L, Hui S, Dongyue C, Xinjun Y, and Jisheng Z (2013a) miR-203 inhibits proliferation of HCC cells by targeting survivin. *Cell Biochem Funct* **31:**82–85.

Wei X, Xiang T, Ren G, Tan C, Liu R, Xu X, and Wu Z (2013b) miR-101 is down-regulated by the hepatitis B virus x protein and induces aberrant DNA methylation by targeting DNA methyltransferase 3A. *Cell Signal* **25:**439–446.

Wietholtz H, Marschall HU, Sjövall J, and Matern S (1996) Stimulation of bile acid 6 alpha-hydroxylation by rifampin. *J Hepatol* **24:**713–718.

Wu X and Brewer G (2012) The regulation of mRNA stability in mammalian cells: 2.0. *Gene* **500:**10–21.

Yang T, Zheng ZM, Li XN, Li ZF, Wang Y, Geng YF, Bai L, and Zhang XB (2013) MiR-223 modulates multidrug resistance via downregulation of ABCB1 in hepatocellular carcinoma cells. *Exp Biol Med (Maywood)* **238:**1024–1032.

Zamek-Gliszczynski MJ, Hoffmaster KA, Nezasa K, Tallman MN, and Brouwer KL (2006) Integration of hepatic drug transporters and phase II metabolizing enzymes: mechanisms of hepatic excretion of sulfate, glucuronide, and glutathione metabolites. *Eur J Pharm Sci* **27:** 447–486.

**Address correspondence to:** Dr. Melissa Runge-Morris, Institute of Environmental Health Sciences, 259 Mack Avenue, Room 5148, Wayne State University, Detroit, MI 48201. E-mail: m.runge-morris@wayne.edu